**Ch8 Inverse Scattering Problems**

Reference: Weng Cho Chew, Waves and Fields in Inhomogeneous Media, IEEE Press, 1994

**8.1 Inverse problem**

Inverse problems are quite important in many problems in physics. In general, inverse problem is a technique where we estimate physical parameters from measured data sets, which cannot directly measure the physical parameters, but it measures the parameters indirectly. The condition can be mathematically expressed as:

$$g(y) = L(f(x)) + n \qquad (8.1.1)$$

where $f(x)$ is a physical parameters to be estimated, $g(y)$ is the measured data set, $L$ is the operator which correlate the physical parameters to the measurable data set and $n$ is the random noise. Here, the operator $L$ and measured data $g(x)$ is known, then the inverse problem estimates the parameters $g(x)$.

There are many examples of inverse problems in geophysics and medical engineering. Most of the geophysical explorations are inverse problems, where the sensors can be put on the ground surface and we estimate the location of mineral resources such as oil. Medical check by a doctor is also one kind of inverse problems, where the doctor measure or observe the patient from outside the body, and estimate the origin of the disease. In remote sensing, radar system is equipped on a space craft or an airplane, and measures the radar signal reflected from the objects on the ground surface. We will estimate the ground surface condition form the radar echo, so it is also one kind of inverse problems.

**8.2 Green's function**

The Green's function of a wave equation is the solution of the wave equation for a point source. Once the Green's function is found, the solution due to a general source can be obtained by the principle of superposition. For example, to obtain the solution to the scalar wave equation:

$$\left(\nabla^2 + k^2\right)\Psi(\boldsymbol{r}) = s(\boldsymbol{r}) \qquad (8.2.1)$$

we first find a solution to the following equation:

$$\left(\nabla^2 + k^2\right) g(\boldsymbol{r},\boldsymbol{r}') = -\delta(\boldsymbol{r} - \boldsymbol{r}') \qquad (8.2.2)$$

Since an arbitrary source $s(\boldsymbol{r})$ is give by:

$$s(\boldsymbol{r}) = \int d\boldsymbol{r}' s(\boldsymbol{r}')\delta(\boldsymbol{r} - \boldsymbol{r}') \qquad (8.2.3)$$

we can obtain the solution to (8.2.1) by using (8.2.2) and (8.2.3) as:

$$\Psi(\boldsymbol{r}) = -\int_V d\boldsymbol{r}' g(\boldsymbol{r},\boldsymbol{r}')s(\boldsymbol{r}') \qquad (8.2.4)$$

The green's functions for simple cases can be found. For example, in homogeneous medium, the solution of (8.2.2) is

given as:

$$g(\boldsymbol{r},\boldsymbol{r}') = g(\boldsymbol{r}-\boldsymbol{r}') = \frac{e^{-jk|\boldsymbol{r}-\boldsymbol{r}'|}}{4\pi|\boldsymbol{r}-\boldsymbol{r}'|} \qquad (8.2.5)$$

**8.3 Inverse Scattering Problems**

In (8.1.1), $L$ can be any kinds of operators, but it is normally determined by a physical theory, such as heat transfer or diffusion equations. When the operator $L$ is related to wave propagation, the problem is called inverse scattering problems. Therefore, the inverse scattering problems include various problems related to electromagnetic wave, acoustic wave and elastic wave propagation, scattering and refraction.

As an example of the operator $L$, now we think about a scalar wave case. The scalar wave equation is given as:

$$\left[\nabla^2 + k^2(r)\right]\phi(r) = q(r) \quad (8.3.1)$$

where

$$k^2(r) = \omega^2\mu(r)\varepsilon(r) \qquad (8.3.2)$$

represents an inhomogeneoius medium over the finite volume and

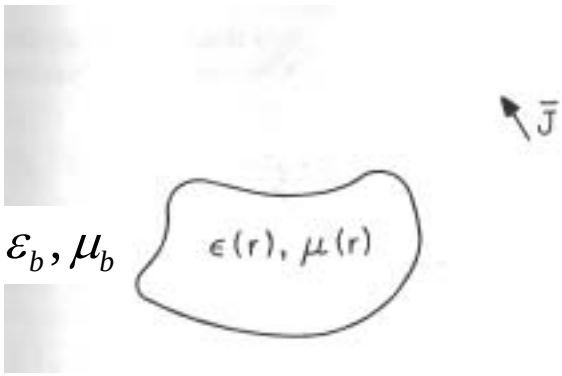


$$k^2 = k_b^2 = \omega^2\mu_b\varepsilon_b \qquad (8.3.3)$$

out side $V$.

Next we define a Green's function satisfying

$$\left[\nabla^2 + k_b^2\right]g(r,r') = -\delta(r-r') \qquad (8.3.3)$$

Then (8.3.1) can be rewritten as

$$\left[\nabla^2 + k_b^2\right]\phi(r) = q(r) - \left[k^2(r) - k_b^2\right]\phi(r) \qquad (8.3.4)$$

Note that the right-hand side of (8.3.4) can be considered as an equivalent source. Then,

$$\phi(r) = -\int_{V_S} dV'\, g(r,r')q(r') + \int_V dV'\, g(r,r')\left[k^2(r) - k_b^2\right]\phi(r') \quad (8.3.5)$$

The first term in the right-hand side is just the field due to the source in the absence of the inhomogeneity, and hence, is the incident field. Therefore, (8.3.5) can be rewritten:

$$\phi(r) = \phi_{inc}(r) + \int_V dV'\, g(r,r')\left[k^2(r) - k_b^2\right]\phi(r') \qquad (8.3.6)$$

In this formulation, we can measure the scattered field $\phi(r)$ in the area outside the volume $V$, and estimate the unknown parameter $k(r)$.

**8.4 Linear Inverse Problems**

We rewrite (8.3.6) as

$$E(r) = E_{inc}(r) + \int_V dr' \bar{G}(r, r') \cdot O(r) E(r') \qquad (8.4.1)$$

where

$$O(r) = k^2(r) - k_b^2 \qquad (8.4.2)$$

is the physical parameter to be estimated.

It should be noted here that in (8.4.1) the field $E(r)$ which should be measured is included both in the left-hand term and in the integral. Therefore, the operator $L$ defined by (8.4.1) for $E(r)$ is a functional of the unknown $O(r)$ to be estimated. This means, the operator is not linear for the unknown, and this is a nonlinear equation. In other words, if the equation is linear, the scattered field $E(r)$ can be expressed as a superposition of the scattered wave caused by each $O(r)$, then it is proportional to $O(r)$.

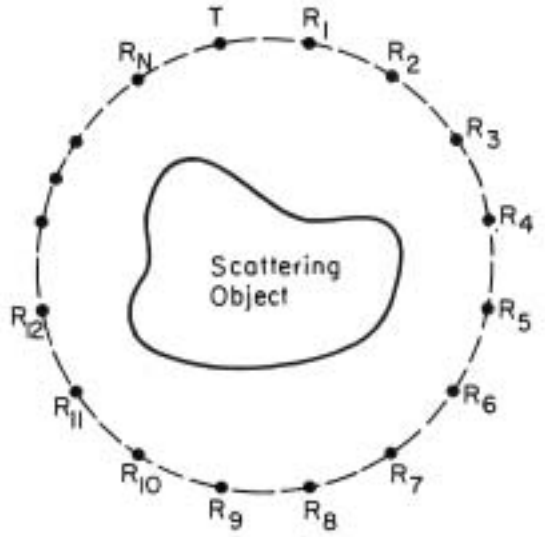


**Figure 9.1.1** An example of an inverse scattering experiment.

The nonlinear dependency of the scattered field on $O(r)$ is due to the mutual interactions between the induced polarization currents. If the scattered field form two isolated scatterers are known, the total scattered field is not a linear superposition of the isolated scattered field as shown in Fig.9.1.2. The multiple scattered fields have to be considered, it causes the nonlinearity of the problem.

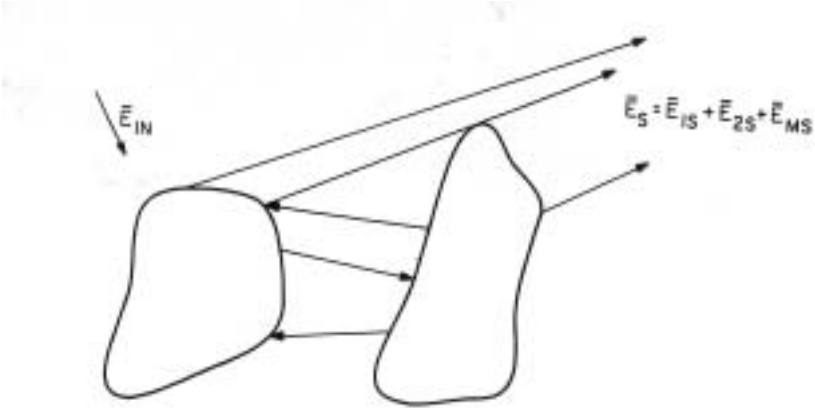


**Figure 9.1.2** Multiple scattering between scatterers gives rise to nonlinearity in the inverse problem which preclude the use of linear superpositions.

However, if we can approximate the problem as a linear problem, we can treat the inverse problem more easily. This is called “linearization” of a problem. There are several conditions, where the problem can be liberalized. For example, in

"Born approximation", the amplitude of the scattered field is linear, whereas, in "Rytov approximation", the phase perturbation is a linear function of objects. Furthermore, another way of obtaining a liberalized relationship between data and the objects is to use high-frequency waves. High-frequency wave propagates in a ray-like manner and with the ray-optics approximation, the relation can be approximately linearlzed. X-ray is such an example.

**8.5 Back-Projection tomography**

The back-projection tomography algorithm is particularly useful when the measured phase or attenuation is linear function of the object, for instance, as in X-ray. The phase shift and attenuation of wave as it propagates through an inhomogeneous medium at high frequency can be given by:

$$e^{-j\omega\int_a^b s(z')dz'} \qquad (8.5.1)$$

The slowness $s(z)$ is complex if the medium is lossy. In X-ray, we measure only the attenuation, and in ultrasound tomography, we measure only the delay of pulse through a body. This delay can be give by:

$$\tau = \int_a^b s(z')dz' \qquad (8.5.2)$$

In both cases, we can assume that the ray propagates along a straight pass, and this assumption stands when the inhomogeneity of the medium is weak.

If the object is described by its slowness or attenuation profile $s(x, y)$, a single experiment then yields

$$P(y') = \int_{-\infty}^{\infty} s(x', y')dx' \qquad (8.5.3)$$

where

where $(x', y')$ are the coordinates of the experiment shown in Fig.9.1.3. $P(y)$ is the projection of the function $s(x', y')$.(8.5.3) can be related to two-dimensional Fourier transformation as

$$s(x', y') = \frac{1}{(2\pi)^2}\iint dk_x' dk_y' e^{-jk_x'x' - jk_y'y'} S(k_x', k_y') \qquad (8.5.5)$$

Then

$$P(y') = \frac{1}{(2\pi)^2}\int_{-\infty}^{\infty} dk_y' e^{-jk_y'y'} S(0, k_y') \quad (8.5.6)$$

Hence, froma single projection, a slice of the Fourier transform of $s(x, y)$, i.e., $S(x', y')$ at $k_x' = 0$, is derivable by inverse Fourier transforming (8.5.6). This is known as the projection-slice theorem. Consequently,

$$S(0, k_y') = \int_{-\infty}^{\infty} dy' e^{+jk_y'y'} P(y') \qquad (8.5.7)$$

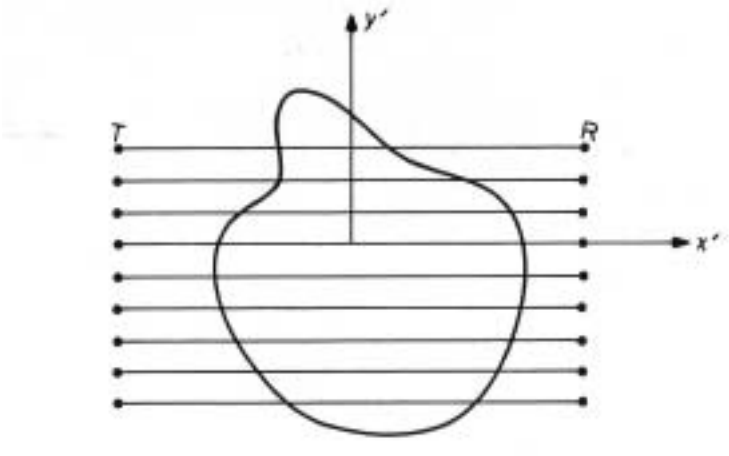


**Figure 9.1.3** A projection tomography measurement scheme.

To get a different slice of the Fourier transform, we need only perform the experiment at a different angle. Therefore, by performing the experiment with angles ranging from $0°$ to $180°$, $S(k_x, k_y)$ will be filled out in the whole Fourier space.

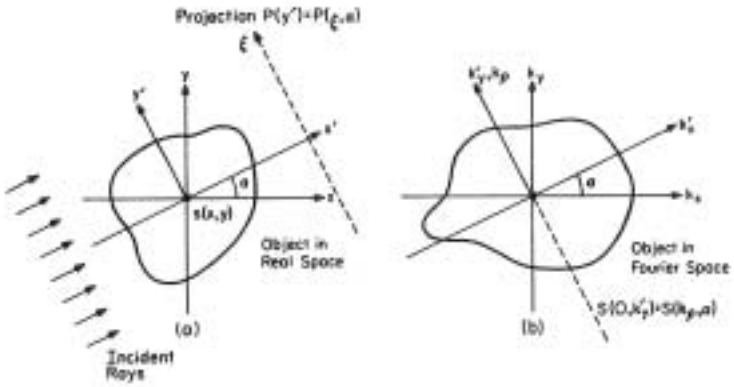


**Figure 9.1.4** The object in real space and in Fourier space. A projection, $P(y') = \int s(x', y')dx'$ is related to $S(0, k'_y)$, a slice in Fourier space.

**8.6 Diffraction tomography**

In projection tomography, we assumed that the wave propagates as straight line ray. However, it is no longer true at longer wavelengths, where diffraction phenomenon is important. Consider a transmitter-receiver configuration as shown in Fig.9.1.5. The scattered field using the first-order Born approximation in a cylindrical coordinate is then:

$$\phi_{sca}(\rho_R) = \int d\rho' \, g(\rho_R, \rho') O(\rho') \phi_{inc}(\rho') \qquad (8.6.1)$$

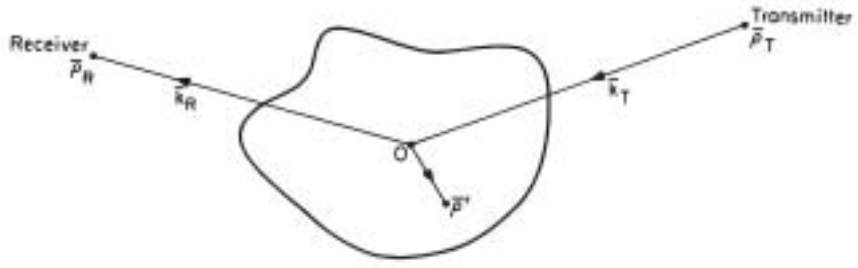


**Figure 9.1.5** A transmitter-receiver measurement in diffraction tomography.

where two-dimensional scattering is assumed and $O(\rho') = k^2 - k_0^2$, is the object to be reconstructed. Moreover, in two dimensions, the Green's function is

$$g(\rho_R, \rho') = \frac{-j}{4} H_0^{(2)}(k_0 |\rho_R - \rho'|) \qquad (8.6.2)$$

But the receiver is in the far field of the scatterer, then approximately,

$$g(\rho_R,\rho') \simeq \frac{-j}{4}\sqrt{\frac{2}{-j\pi k_0\rho_R}}e^{-jk_0\rho_R+jk_0\hat{\rho}_R\cdot\rho'} \qquad (8.6.3)$$

Also, an incident field generated by a uniform line source is

$$\phi_{inc}(\rho') = \frac{-j}{4}H_0^{(2)}(k_0|\rho'-\rho_T|) \qquad (8.6.4)$$

and if the transmitter is also in the far field of the object we have

$$\phi_{inc}(\rho') \simeq \frac{-j}{4}\sqrt{\frac{2}{-j\pi k_0\rho_T}}e^{-jk_0\rho_T+jk_0\hat{\rho}_T\cdot\rho'} \qquad (8.6.5)$$

Finally, after defining $\boldsymbol{k}_R = k_0\hat{\rho}_R$ and $\boldsymbol{k}_T = -k_0\hat{\rho}_T$ and substituting the above into (8.6.1) we have

$$\phi_{sca}(\rho_R) = \frac{-j}{8\pi k_0\sqrt{\rho_T\rho_R}}e^{-jk_0(\rho_T+\rho_R)}\int d\rho' e^{j(\boldsymbol{k}_R-\boldsymbol{k}_T)\cdot\rho'}O(\rho')\phi_{inc}(\rho') \qquad (8.6.6)$$

Note that now, the integral is a Fourier-transform integral. Consequently,

$$\phi_{sca}(\rho_R) = \frac{-j}{8\pi k_0\sqrt{\rho_T\rho_R}}e^{-jk_0(\rho_T+\rho_R)}\tilde{O}(\boldsymbol{k}_R-\boldsymbol{k}_T) \qquad (8.6.7)$$

where $\tilde{O}(\boldsymbol{k})$ is the Fourier transform of $O(\rho)$. Therefore, the scattered field under the Born approximation is related to the Fourier transform of the object.

Observe that the length of the vector $\boldsymbol{k}_R$ and $\boldsymbol{k}_T$ are equal to $k_0$. Hence, $\boldsymbol{k}_R-\boldsymbol{k}_T$ or the argument of $\tilde{O}$, can only span a finite space in the Fourier space. For instance, if $\boldsymbol{k}_T$ is fixed and the receiver is moved around so that $\boldsymbol{k}_R$ change directions, then the locus swept out by $\boldsymbol{k}_R-\boldsymbol{k}_T$ is as shown in Fig. 9.1.6. Furthermore, if the transmitter is moved around so that $\boldsymbol{k}_T$ changes directions as well as $\boldsymbol{k}_R$, then the combination of varying the directions of $\boldsymbol{k}_R$ and $\boldsymbol{k}_T$ sweeps out a larger circle of radius $2k_0$ with are a. $4\pi k_0^2$.

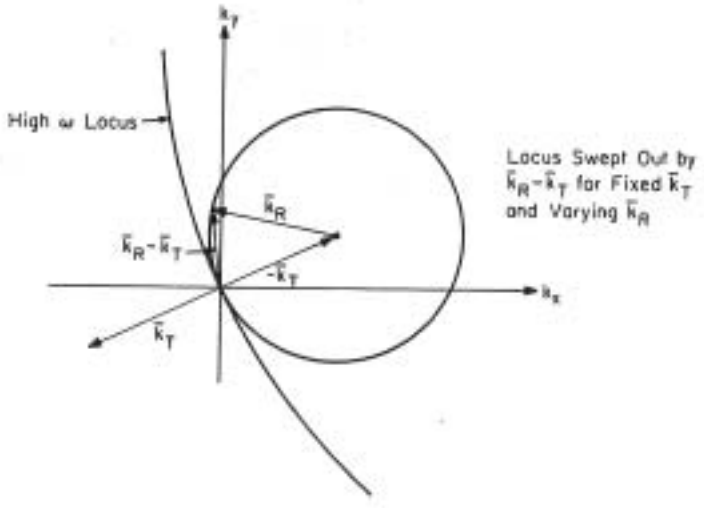


**Figure 9.1.6** Locus swept out by $\mathbf{k}_R-\mathbf{k}_T$ for a fixed $\mathbf{k}_T$ and varying $\mathbf{k}_R$.

It should be noted that we can acquire the Fourier spectrum of $\tilde{O}(\boldsymbol{k})$ only for $|\boldsymbol{k}| \le k_0$, only a low-pass version of $\tilde{O}(\boldsymbol{k})$ is retrieved in this reconstruction.

It is interesting to note that when the frequency becomes very high, the locus of $\boldsymbol{k}_R - \boldsymbol{k}_T$ passes through the origin almost like a straight line, as shown in Fig. 9.1.6. This means, that we can understand that the projection tomography using the projection-slice theorem is a special case of diffraction tomography. Hence, in the high-frequency limit, we need only a sweep of receiver with a small angle, and a straight-line slice in the Fourier space is recovered.

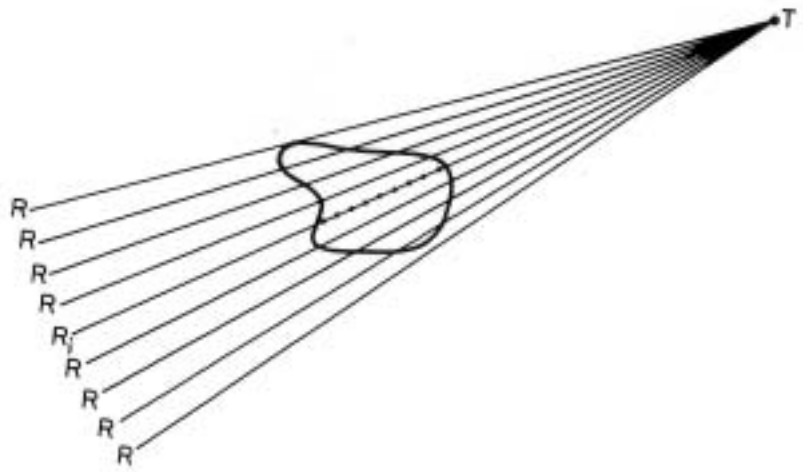


**Figure 9.1.7** The limit when diffraction tomography becomes projection tomography.

**8.7 Finite-Source Effect**

In the previous section, we used a far0field approximation. The far-field approximation is valid only when

$$\rho_T \gg \rho', \rho_R \gg \rho' \quad (8.7.1)$$

or the transmitter and the receiver are far from the size of the scatterer. However, it is not true for many GPR measurements. If we do not use the far-field approximation, (8.6.4) can be expanded by using a plane wave expansion of Hankel function, we have:

$$\phi_{inc}(\rho') \simeq \frac{-j}{4\pi} \int_{-\infty}^{\infty} dk_x \frac{1}{k_y} e^{-jk_x(x'-x_T)-jk_y|y'-y_T|} \quad (8.7.2)$$

Similarly, the Green's function can be represented as:

$$g(\rho, \rho') \simeq \frac{-j}{4\pi} \int_{-\infty}^{\infty} dk_x' \frac{1}{k_y'} e^{-jk_x'(x_R-x')-jk_y'|y_R-y'|} \quad (8.7.3)$$

Consequently, substituting (8.7.2) and (8.7.3) into (8.6.1) we have:

$$\phi_{sca}(\rho_R,\rho_T)=\frac{-1}{16\pi^2}\int_{-\infty}^{\infty}\frac{dk_x}{k_y}\int_{-\infty}^{\infty}\frac{dk_x'}{k_y'}e^{-jk_x'x_R+jk_xx_T}\int dx'dy'e^{-j(k_x-k_x')x'-jk_y'|y'-y_T|-jk_y'|y_R-y'|}O(x',y') \tag{8.7.4}$$

Note that the scattered field is a function of both the transmitter and the receiver positions. But in forward scattering experiments, $y'>y_T$ and $y_R>y'$ so that the modulus signs in (8.7.4) can be removed to arrive at

$$\phi_{sca}(\rho_R,\rho_T)=\frac{-1}{16\pi^2}\int_{-\infty}^{\infty}\frac{dk_x}{k_y}\int_{-\infty}^{\infty}\frac{dk_x'}{k_y'}e^{-jk_x'x_R-jk_y'y_R-jk_xx_T+jk_yy_T}\int dx'dy'e^{-j(k_x-k_x')x'-j(k_y-k_y')y'}O(x',y') \tag{8.7.5}$$

Now, if $\phi_{sca}(\rho_R,\rho_T)$ is measured along a line in the x direction, with the transmitter also aligned in the x direction as shown in Fig. 9.1.8, we can transform $\phi_{sca}(\rho_R,\rho_T)$ in the $x_R$ and $x_T$ variables to obtain

$$\phi_{sca}(k_x',y_R,-k_x,y_T)=\frac{-1}{4}\frac{e^{-jk_y'y_R+jk_yy_T}}{k_yk_y'}O(-k_x+k_x',-k_y+k_y') \tag{8.7.6}$$

In this case, the Fourier transform of the measured field is related to the Fourier transform of the object $\tilde{O}$.

From (8.7.6), note that one cannot make much use of the evanescent spectrum corresponding to the case when $k_y$ and $k_y'$ are purely imaginary. This happens when $k_x>k_0$ and $k_x'>k_0$, as seen from the dispersion relationships $k_x'^2+k_y'^2=k_0^2$ and $k_x^2+k_y^2=k_0^2$. Therefore, it is reasonable to assume that the direction of $\boldsymbol{k}$ and $\boldsymbol{k'}$ only sweep from $0°$ to $180°$. Since $\tilde{O}$ is a function of $\boldsymbol{k'-k}$, the locus swept out by $\boldsymbol{k'-k}$ with varying $\boldsymbol{k'}$ for a fixed $\boldsymbol{k}$ is as shown in Fig. 9.1.9. Therefore, a forward scattering experiment alone is not enough to reconstruct the object well since the data in the spectral domain is not complete. Nevertheless, a band-limited reconstruction is possible.

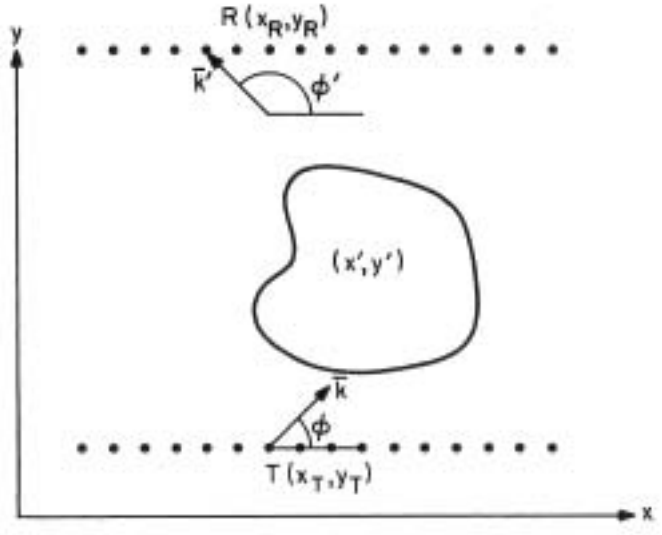


**Figure 9.1.8** The finite-source effect in diffraction tomography.

On the other hand, if a back scattering experiment is performed instead, only the sings of $k_y^{'}$ in (8.7.6) need to be changes. In this case, the area swept out by $\boldsymbol{k'-k}$ includes a semicircular as well in the lower half $k_x k_y$ plane. To fill out a full circle, the experimental setting is rotated so that the two discs sweep out a circle of radius $2k_0$. Alternatively, the transmitters and receivers can be switched to sweep out a full circle on the $k_x k_y$ plane. In this matter, more Fourier data can be collected in the Fourier space.

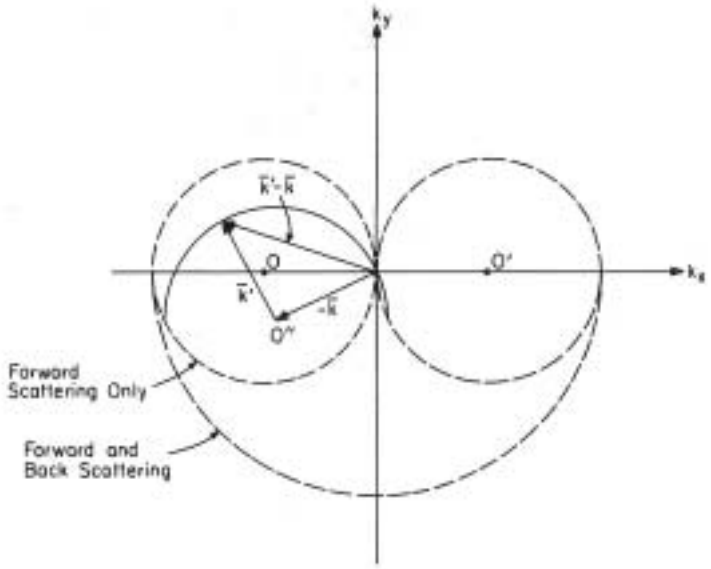


**Figure 9.1.9** Locus swept out in the **k**-space in a forward and backward scattering experiment only.